Eur. J. Mech. B - Fluids 20 (2001) 399–414

S0997-7546(00)01122-5/FLA

Steady rise of a small spherical gas bubble along the axis of a cylindrical pipe at high Reynolds number

John D. Sherwood

Schlumberger Cambridge Research, High Cross, Madingley Road, Cambridge CB3 0EL, UK

(Received 29 May 2000; revised and accepted 23 November 2000)

Abstract – Steady irrotational flow of inviscid liquid of density ρ_l around a spherical gas bubble which lies on the axis of a cylindrical pipe is investigated using the analysis of Smythe (Phys. Fluids 4 (1961) 756). The bubble radius $b = qa$ is assumed small compared to the pipe radius a, and the interfacial tension between gas and liquid is γ. Far from the bubble, in the frame in which the bubble is at rest, the liquid velocity along the pipe is v_0, whereas the liquid velocity at points on the wall closest to the bubble is $U_{zw} = v_0(1 + 1.776q^3 + \cdots)$. The decrease in wall pressure as the bubble passes is therefore $\Delta p = 1.776\rho_l v_0^2 q^3$. When the Weber number $W = 2bv_0^2\rho_l/\gamma$ is small, the bubble deforms into an oblate spheroid with aspect ratio $\chi = 1 + 9W(1 + 1.59q^3)/64$. If the fluid viscosity μ is non-zero, and the Reynolds number $\mathrm{Re} = 2v_0\rho_l b/\mu$ is large, a viscous boundary layer develops on the walls of the pipe. This decays algebraically with distance downstream of the bubble, and an exponentially decaying similarity solution is found upstream. The drag D on the bubble is $D = 12\pi\mu v_0 b(1 - 2.21\mathrm{Re}^{-1/2})(1 + 1.59q^3) + 7.66\mu v_0 b\mathrm{Re}^{1/2}q^{9/2}$, larger than that given by Moore (J. Fluid Mech. 16 (1963) 161) for motion in unbounded fluid. At high Reynolds numbers the dissipation within the viscous boundary layers might dominate dissipation in the potential flow away from the pipe walls, but such high Reynolds numbers would not be achieved by a spherical air bubble rising in clean water under terrestrial gravity. © 2001 Éditions scientifiques et médicales Elsevier SAS

gas bubble / inviscid liquid

1. Introduction

The translation of bubbles relative to surrounding liquid plays an important role in many chemical engineering processes. The surrounding liquid is usually bounded by container walls or by free surfaces, and bubble motion will be affected if the bubbles are close to these boundaries. The translation of a gas bubble along the centre-line of a pipe is one of the simplest examples of interaction between a bubble and a rigid wall. Here we study steady potential flow of inviscid liquid around a spherical bubble translating with velocity v_0 along the axis of a circular tube. The original motivation for the work presented here comes from investigations of laminar gas-liquid flow through a vertical Venturi [1,2].

Steady potential flow of inviscid fluid around a sphere translating with velocity v_0 along the axis of a circular tube has been studied by Smythe [3,4] and by Cai and Wallis [5]. Cai and Wallis present an asymptotic analysis for the added mass of a sphere which nearly fills the tube. Here we study the opposite limit, in which the sphere radius b is small compared to the radius a of the pipe. The liquid is incompressible with density ρ_l. The far field around a sphere translating in unbounded fluid is a dipole and we expect the flow field to be only slightly perturbed by the distant pipe walls. Nevertheless an estimate of this perturbation is useful in order to check (and correct for) the effect of finite computational domains in numerical computations.

E-mail address: sherwood@cambridge.scr.slb.com (J. Sherwood).

Potential flow around a sphere has been used by Hartunian and Sears [6] and by Moore [7,8] as the basis for predicting the deformation of a gas bubble in terms of the Weber number

$$W = 2bv_0^2\rho_l/\gamma, \tag{1}$$

where γ is the interfacial tension between gas and liquid. If the bubble is rising under gravity the velocity v_0, and hence the deformation, depends upon the Morton number [9]

$$M = \frac{g\mu^4}{\rho_l\gamma^3}, \tag{2}$$

where $\mu = \nu\rho_l$ is the fluid viscosity and g the acceleration due to gravity. Moore [8] considered the bubble deformation to be no longer small when the bubble aspect ratio $\chi > 1.05$. This occurs when the bubble Reynolds number

$$\mathrm{Re} \equiv 2bv_0\rho_l/\mu = 1.1M^{-1/5}. \tag{3}$$

For an air bubble in clean water $M \approx 2.4 \times 10^{-11}$, so that the Reynolds number corresponding to a 5% deformation is $\mathrm{Re} = 150$. In section 4 we will discuss how the deformation of a spherical bubble is changed by the presence of the pipe walls.

Potential flow around a sphere has also been used as the basis for computations of the high Reynolds number drag on a spherical bubble, even though in reality the flow will not be irrotational at the surface of the bubble, where a weak boundary layer will develop [10]. Levich [11] assumed that at high Reynolds numbers the velocity field around a bubble translating in unbounded liquid can be approximated by potential flow, and he computed the total rate of dissipation in the liquid. The rate of working Dv_0 of the drag D acting on the bubble must equal the total rate of dissipation, and hence

$$D = 12\pi\mu bv_0. \tag{4}$$

The Levich drag (4) was eventually obtained directly by integration of the stress acting on the bubble by Kang and Leal [12]. Moore [10] considered the effect of dissipation within the boundary layer over the surface of the bubble and the bubble wake, and obtained

$$D = 12\pi\mu bv_0\left[1 - \frac{2.21}{\mathrm{Re}^{1/2}} + \mathrm{O}\left(\mathrm{Re}^{-5/6}\right)\right], \tag{5}$$

where the $\mathrm{O}(\mathrm{Re}^{-5/6})$ corrections come from the region around the rear stagnation point.

Experimental investigations of the effect of pipe diameter on the bubble drag, and hence on its rate of rise, are reviewed by Clift et al. [13]. When $\mathrm{Re} > 200$ the effect of the pipe is independent of Reynolds number. Empirical correlations have suggested that if the rate of rise of a bubble in unbounded fluid is v_0^∞, experimental data for the rise velocity v_0 in a pipe of radius a can be fitted by a curve of the form

$$v_0 = v_0^\infty\left[1 - q^2\right]^{3/2}, \tag{6}$$

where

$$q = b/a. \tag{7}$$

Recent experiments and reviews [14] have used (6) in order to correct for the effect of an outer boundary.

Numerical computations of the flow around spherical bubbles usually investigate motion in unbounded fluid (e.g. [15]), sometimes by applying an appropriate boundary condition far from the bubble (e.g. [16]). Magnaudet et al. [17] performed computations in a cylindrical domain. Though they checked that the outer boundary was sufficiently far from the sphere that its exact position was unimportant, they do not give details of the rate at which the drag D acting on a bubble converges to its value in unbounded fluid.

In section 5 we use the potential flow, as perturbed by the presence of the pipe, to compute the perturbation to the rate of energy dissipation and hence the perturbation to the drag (5). We shall find that the predicted perturbation to the drag is markedly smaller than that observed in the experimental correlation (6). One additional source of dissipation in experiments is the viscous boundary layer on the pipe walls. The effect of this will be discussed in section 6.

We note in passing that when the bubble is small the interaction between the pipe and the dipole far field around a translating bubble leads to a small perturbation. This differs from the case of a monopole oscillation of a bubble [2,18] in which the pipe walls can drastically modify the frequency of oscillation of a bubble, even if $b \ll a$.

2. Governing equations

Smythe [3] studied potential flow around a sphere of radius b at rest on the axis of a pipe (*figure 1*). The pipe axis is in the z direction and the pipe walls are at $\rho = a$, where (ρ, ϕ, z) are cylindrical coordinates with the centre of the sphere at $\rho = z = 0$. Smythe determined a vector potential A_ϕ such that the fluid velocity is $\boldsymbol{u} = (u_\rho, 0, u_z) = \nabla \wedge (A_\phi \boldsymbol{e}_\phi)$, where $\boldsymbol{e}_\phi$ is a unit vector in the ϕ direction. Thus in cylindrical coordinates

$$u_\rho = -\frac{1}{\rho}\frac{\partial(\rho A_\phi)}{\partial z}, \qquad u_z = \frac{1}{\rho}\frac{\partial(\rho A_\phi)}{\partial \rho}. \tag{8}$$

Smythe [3] wrote the vector potential A_ϕ in the form

$$A_\phi = A_\phi^{(1)} + A_\phi^{(2)} + A_\phi^{(3)}, \tag{9}$$

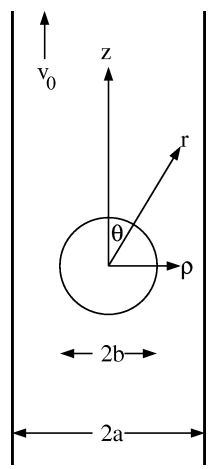

Figure 1. The sphere of radius $b = qa$ on the centreline of a pipe of radius a.

where $A_\phi^{(1)} = \frac{1}{2}v_0\rho$ corresponds by (8) to uniform flow of liquid with velocity

$$u_z^{(1)} = v_0. \tag{10}$$

The term $A_\phi^{(2)}$ in (9) is expanded as

$$A_\phi^{(2)} = \sum_{n=0}^{\infty} \frac{bv_0C_n}{4n+3}\left(\frac{r}{b}\right)^{2n+1} P_{2n+1}^1(\cos\theta) \quad r < b \tag{11a}$$

$$= \sum_{n=0}^{\infty} \frac{bv_0C_n}{4n+3}\left(\frac{b}{r}\right)^{2n+2} P_{2n+1}^1(\cos\theta) \quad r > b, \tag{11b}$$

where P_{2n+1}^1 is a Legendre polynomial and (r, θ, ϕ) are spherical polar coordinates based on the centre of the sphere, with $\theta = 0$ corresponding to the z axis. Smythe [3] showed that the choice

$$A_\phi^{(3)} = \sum_{n=0}^{\infty} \frac{(-1)^{n+1}2v_0C_nb^{2n+3}}{\pi(4n+3)(2n)!} \int_0^\infty \frac{t^{2n+1}K_1(ta)I_1(t\rho)\cos(tz)}{I_1(ta)}\,\mathrm{d}t \tag{12}$$

with K_1, I_1 modified Bessel functions, ensures zero flow normal to the wall of the tube at $\rho = a$. Smythe truncated the expansions (11), (12) at $n = N$, ensuring that N was sufficiently large that the precise choice of N did not affect the solution. The vector potential must be constant on the surface of the sphere, since this is a streamline, and it vanishes everywhere within the sphere if the C_n satisfy the $N + 1$ equations

$$\frac{\delta_{p0}}{2} = \frac{2(4p+3)q^3}{3\pi(2p+2)!}\sum_{n=0}^{N} \frac{(-q^2)^{n+p}C_nI(2n+2p+2)}{(4n+3)(2n+2p+3)(2n)!} - \frac{C_p}{3}, \quad 0 \leqslant p \leqslant N. \tag{13}$$

Values for $(s!)^{-2}I(2s) = (s!)^{-2}\int_0^\infty t^{2s}[I_1(t)]^{-2}\,\mathrm{d}t$ are given in table 1 of [4], which corrects minor errors in table 1 of [3]. In particular $I(2s) = 7.5098907$ when $s = 1$.

In the limit $q = b/a \to 0$ we find from (13) that $C_n = \mathrm{O}(q^{2n+3})$ for $n \geqslant 1$ and will be considered negligibly small from here on, whereas

$$C_0 = -\frac{3}{2}\left(1 - \frac{I(2)q^3}{3\pi}\right)^{-1} = -\frac{3}{2}G, \tag{14}$$

where

$$G = 1 + 0.796824151q^3 + \cdots. \tag{15}$$

When $q = 0.1$ we obtain $C_0 = -1.5011952$, in agreement with the tabulated values of [4]. Cai and Wallis [5] showed that the added mass coefficient C_{am} of the sphere is $C_{\mathrm{am}} = -C_0 - 1$. Hence

$$C_{\mathrm{am}} = -C_0 - 1 = \frac{1}{2} + 1.195q^3 + \cdots, \quad q \ll 1, \tag{16}$$

a result which would seem to be new.

3. Velocity and pressure fluctuations at the wall

The pressure on the pipe wall will vary as the bubble passes by, and in order to determine this change we evaluate the liquid velocity U_{zw} at the pipe wall. Smythe [3] gives an expansion valid for $z \gg a$:

$$A_\phi = v_0\left[\frac{\rho}{2} + \sum_{r=1}^{\infty} D_r J_1(k_r\rho)\mathrm{e}^{-k_r z}\right], \tag{17}$$

where the k_r are roots of $J_1(k_r a) = 0$ and

$$D_r = \frac{2b^3}{a^2 J_0^2(k_r a)} \sum_{n=0}^{N} \frac{(k_r b)^{2n} C_n}{(4n+3)(2n)!} \approx \frac{2b^3 C_0}{3a^2 J_0^2(k_r a)}. \tag{18}$$

Hence, by (8), (17) and (18)

$$U_{zw} = v_0 + v_0 \sum_{r=1}^{\infty} \frac{2b^3 C_0 k_r \mathrm{e}^{-k_r z}}{3a^2 J_0(k_r a)}, \quad z \gg a. \tag{19}$$

This expression does not converge when $z = 0$, and we instead look for an expansion which is valid for $z \ll a$.

It is straightforward to differentiate the potential $A_\phi^{(2)}$ to find that on the wall $\rho = r\sin\theta = a$

$$u_z^{(2)} = u_r^{(2)}\cos\theta - u_\theta^{(2)}\sin\theta = \frac{v_0 C_0 b^3(2z^2 - a^2)}{3(a^2+z^2)^{5/2}}, \tag{20}$$

where $u_r^{(2)}$ and $u_\theta^{(2)}$ are velocity components expressed in spherical coordinates. Smythe shows that when $z \ll a$, $A_\phi^{(3)}$ may be expressed as an expansion in powers of ρ and z:

$$\begin{aligned} A_\phi^{(3)} &= \frac{2v_0}{\pi} \sum_{n=0}^{N} \frac{(-1)^{n+1} C_n b^{2n+3}}{(4n+3)(2n)!} \int_0^\infty \frac{t^{2n+1} K_1(ta)}{I_1(at)} \left[\sum_{k=0}^{\infty} \frac{(t\rho)^{2k+1}}{2^{2k+1}k!(k+1)!} \sum_{r=0}^{\infty} \frac{(-t^2 z^2)^r}{(2r)!}\right] \mathrm{d}t \\ &= \frac{2v_0}{\pi} \sum_{n=0}^{N} \sum_{r=0}^{\infty} \sum_{k=0}^{\infty} \frac{(-1)^{n+1+r} C_n b^{2n+3} I(2n+2k+2+2r) z^{2r} \rho^{2k+1}}{(4n+3)(2n)! a^{2n+2k+3+2r} 2^{2k+1} k!(k+1)!(2n+2k+3+2r)(2r)!}. \end{aligned} \tag{21}$$

Setting $C_n = 0$ for $n \geqslant 1$ we obtain a contribution to the wall velocity

$$u_z^{(3)} = \frac{2v_0 C_0}{3\pi}\left(\frac{b}{a}\right)^3 \sum_{r=0}^{\infty} \sum_{k=0}^{\infty} \frac{(-1)^{1+r} I(2k+2+2r)(2k+2)}{2^{2k+1}k!(k+1)!(2k+3+2r)(2r)!}\left(\frac{z}{a}\right)^{2r}. \tag{22}$$

Summing this numerically using the values of I tabulated by Smythe [4], we find

$$u_z^{(3)} = -C_0 v_0\left(\frac{b}{a}\right)^3 \left[0.85052 - 2.0840(z/a)^2 + 3.7859(z/a)^4 + \cdots\right]. \tag{23}$$

Adding (10), (20) and (23) and using (14), we obtain the wall velocity

$$U_{zw} = v_0 + v_0\left(\frac{b}{a}\right)^3 \left[1.77578 - 5.67885(z/a)^2 + 10.36635(z/a)^4 + \cdots\right] \tag{24}$$

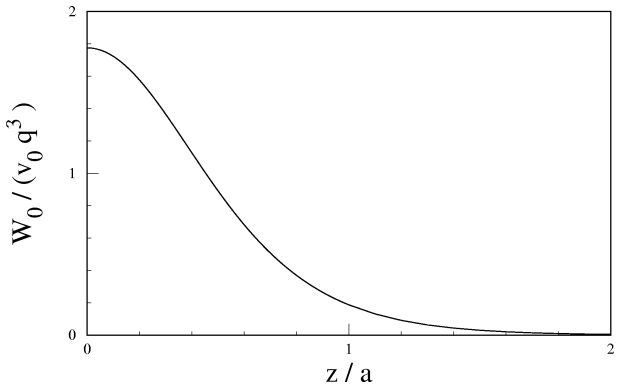

Figure 2. The perturbation W_0 to the liquid velocity at the wall in the frame in which the sphere is at rest, as a function of axial position z from the centre of the sphere.

in the limit $q \ll 1$. The correction to the wall velocity due to the presence of the bubble is

$$W_0 = U_{zw} - v_0 \tag{25}$$

and this is shown (after scaling by $v_0 q^3$) in *figure 2*. For comparison, we note from the stream function given in [19] that at $(z = 0, r = a)$ the velocity around a sphere in unbounded fluid is $u_z = v_0 + 0.5 v_0 (b/a)^3$.

The liquid velocity at the wall far from the bubble is $U_{zw} = v_0$, whereas the velocity at the wall at $z = 0$ is given by (24). Bernoulli's equation therefore predicts that the wall pressure decreases by an amount

$$\Delta p = 1.77578 \rho_l v_0^2 q^3 \tag{26}$$

as the bubble goes past a wall pressure sensor.

4. Bubble deformation

We now consider the liquid velocity over the surface of the spherical bubble in order to find a correction to the shape of the bubble. The vector potential is zero (by construction) throughout the interior of the sphere, so that the tangential velocity just within the sphere due to the sum of $A_\phi^{(1)}$ and $A_\phi^{(3)}$ is equal and opposite to that due to $A_\phi^{(2)}$ (11a). But derivatives of $A_\phi^{(1)} + A_\phi^{(3)}$ are continuous at the surface of the sphere, so the tangential velocity just outside the surface of the sphere is

$$u_\theta = -\left(\frac{b v_0 C_0 \sin\theta}{3}\right) \frac{1}{r} \frac{\partial}{\partial r} \left[\frac{b^2}{r} - \frac{r^2}{b}\right] = v_0 C_0 \sin\theta = -\frac{3}{2} v_0 G \sin\theta. \tag{27}$$

Higher order spherical harmonics due to the terms C_n $(n \geqslant 1)$ in (11) are $O(q^5)$ and have been ignored. The tangential velocity on the surface of a sphere in unbounded flow is $v_\theta = -\frac{3}{2} v_0 \sin\theta$, which differs from (27) only by a factor G (15). Small deformations of the bubble can therefore be found immediately from the equivalent deformation of a bubble rising in unbounded fluid. This was obtained by Hartunian and Sears [6] but is conveniently to be found in [7]. The bubble in a pipe becomes an oblate spheroid of the form

$$r = b\left[1 + \varepsilon P_2(\cos\theta)\right] \tag{28}$$

with

$$\varepsilon = -\frac{3}{16}\left(\frac{v_0^2 b\rho_l}{\gamma}\right)G^2. \tag{29}$$

In terms of the Weber number W (1) and the ratio χ of the transverse to longitudinal axes of the bubble, we have

$$\chi = 1 + \frac{9}{64}WG^2. \tag{30}$$

5. The dissipation in the irrotational core and bubble boundary layer

5.1. Dissipation in the irrotational core

We first study how the change in potential flow caused by the presence of the pipe affects the energy dissipation in the irrotational core, in order to obtain a correction to the Levich drag (4). In section 5.2 we shall examine the effect of the pipe upon the dissipation within the bubble boundary layer and wake in order to obtain a correction to Moore's drag (5).

In potential flow the fluid velocity $\boldsymbol{u} = \nabla\Phi$, where the potential Φ satisfies the Laplace equation, and the rate of strain is $e_{ij} = \frac{1}{2}(\partial u_i/\partial x_j + \partial u_j/\partial x_i) = \partial^2\Phi/\partial x_i\partial x_j$. The rate of viscous dissipation over the total volume of liquid V_l is

$$\frac{\mathrm{d}E}{\mathrm{d}t} = 2\mu\int_{V_l} e_{ij}e_{ij}\,\mathrm{d}V = 2\mu\int_{S_l} n_i u_j\frac{\partial u_i}{\partial x_j}\,\mathrm{d}S, \tag{31}$$

where $\boldsymbol{n}$ is the normal directed out of V_l and S_l is the boundary of V_l. If $\boldsymbol{n}$ is constant along streamlines on the boundary (as occurs here on the pipe walls) then

$$n_i u_j\frac{\partial u_i}{\partial x_j} = u_j\frac{\partial}{\partial x_j}(n_i u_i) \tag{32}$$

and this is zero on the tube walls since $\boldsymbol{n}\cdot\boldsymbol{u} = 0$. Consider a surface S_l which includes the pipe walls, the surface of the bubble, and two discs of liquid far upstream and downstream of the bubble. The integral (31) over the pipe wall is zero, and the integrals over the discs decay as these move to infinity. All that remains is the contribution from the surface S_b of the bubble. In the frame of reference in which the bubble is at rest the liquid velocity on the surface of the bubble is given by (27), so that $\boldsymbol{u}\cdot\nabla = u_\theta\partial/\partial\theta$. Noting that $\partial\hat{\boldsymbol{\theta}}/\partial\theta = -\hat{\boldsymbol{r}}$, where $\hat{\boldsymbol{r}}$ and $\hat{\boldsymbol{\theta}}$ are unit vectors in the (r,θ) directions, the integral over the surface of the bubble is found to be

$$\frac{\mathrm{d}E}{\mathrm{d}t} = 12\pi\mu b v_0^2 G^2. \tag{33}$$

The rate of energy dissipation must equal the rate at which work is done by the forces acting on the surface S_l. In the frame in which fluid at infinity is at rest no work is done at the liquid discs far upstream and downstream. Similarly no work is done by the pressure acting on the pipe wall, since the fluid velocity normal to the wall is zero. All the work is therefore performed by the drag force D acting on the bubble which moves with velocity v_0, so that

$$D = 12\pi\mu b v_0\left(1 + 1.5936q^3\right) \tag{34}$$

which agrees with the Levich drag (4) in the limit $q \to 0$.

5.2. The boundary layer on the bubble and the bubble wake

Moore [10] discussed the boundary layer on a bubble rising through unbounded fluid. The potential flow around the bubble has a rate of strain $e_{r\theta} = 3v_0 \sin\theta/2b$ on the surface of the bubble, and if the bubble surface is to be stress-free a boundary layer will develop. The vorticity created in this boundary layer is convected downstream and forms a wake behind the bubble. Moore estimated the change in the drag due to the boundary layer and wake by computing the rate of energy dissipation in these two regions.

One immediate effect of the cylindrical boundary is to change the potential flow at the surface of the bubble. The rate of strain at the surface can most easily be obtained in the same manner as in section 4 by noting that the velocity field and rate of strain are identically zero within the sphere. The rate of strain just outside the sphere is then found to be $e_{r\theta} = 3Gv_0 \sin\theta/2b$, so that the velocities within the boundary layer are increased by a factor G. The dissipation is increased by a factor G^2.

The vorticity within the wake is similarly increased by a factor G, so that Moore's energy dissipation within both the bubble and wake are increased by a factor G^2 and Moore's drag (5) therefore increases to

$$D = 12\pi\mu b v_0 \left(1 - \frac{2.21}{\mathrm{Re}^{1/2}}\right)(1 + 1.5936q^3). \tag{35}$$

However, the velocity field within the wake will also be modified by the presence of the cylindrical walls of the pipe. Moore [10] assumes that the perturbation velocity q_z within the wake decays to zero as $\rho \to \infty$, and integrates his equation (3.27) to find, in unbounded fluid

$$q_z = -6\sqrt{2}v_0\delta\left[\pi^{-1/2}\exp(-\sigma^2) - \sigma\,\mathrm{erfc}\,\sigma\right], \tag{36}$$

where

$$\delta = \left(\frac{\nu}{bv_0}\right)^{1/2} = \left(\frac{2}{\mathrm{Re}}\right)^{1/2} \tag{37}$$

is a scaling for the thickness of the boundary layer on the bubble surface, and

$$\sigma = \frac{\rho^2}{4\sqrt{2}b^2\delta}. \tag{38}$$

In the pipe considered here we require that the total volumetric flow rate across the pipe cross-section is unperturbed. Noting that just behind the bubble the wake diameter is small compared to that of the cylinder, we may integrate Moore's (3.27) and satisfy zero volumetric flow by adding a uniform backflow $12v_0\delta^2q^2$ to the right-hand side of (36), so that $\int_0^\infty q_z\rho\,\mathrm{d}\rho = 0$. Moore's subsequent analysis for the wake can be adapted for the bounded cylindrical geometry with very little modification. The boundary condition at $\rho = a$ can be either a no-slip condition $q_z = 0$ (with a boundary layer) or a stress-free condition $\partial q_z/\partial\rho = 0$ such as might be adopted when performing numerical computations in a large but bounded domain intended to represent unbounded fluid. The backflow leads to a perturbation to the drag which scales as $\mu v_0 b\mathrm{Re}^{-1}q^2$. One can similarly discuss the displacement thickness of the boundary layer on the surface of the sphere which is $\mathrm{O}(b\delta^2)$. This effectively changes the dimensions of the particle. It should therefore lead to an additional drag term $\mathrm{O}(\mu v_0 b\mathrm{Re}^{-1})$ in unbounded fluid and a correction $\mathrm{O}(\mu v_0 b\mathrm{Re}^{-1}q^3)$ due to the bounding cylindrical container. In the absence of any analysis for the $\mathrm{O}(\mu v_0 b\mathrm{Re}^{-5/6})$ correction to Moore's drag (5) due to the stagnation region behind the bubble, it seems inappropriate to pursue corrections which are $\mathrm{O}(\mathrm{Re}^{-1})$.

6. The viscous boundary layer at the wall

6.1. The boundary layer equation

We now turn to a laboratory coordinate system

$$\zeta = z - v_0 t, \tag{39}$$

in which the pipe walls are stationary, the bubble moves with velocity $-v_0$ and the liquid is at rest at infinity. The liquid velocity at the wall in the potential flow is

$$U_{\zeta w}(\zeta) = U_{zw}(\zeta + v_0 t) - v_0 = W_0. \tag{40}$$

If the fluid is viscous, the potential flow obtained in section 2 will be valid in the interior of the pipe, but a boundary layer will develop at the pipe walls. Far upstream of the bubble the liquid is initially at rest, but an observer at fixed ζ will see the wall velocity outside the boundary layer first increase, and then decrease. Once the bubble has gone past, the vorticity within the boundary layer will diffuse away from the wall. We now estimate the rate of viscous dissipation within this boundary layer.

We assume that the boundary layer is everywhere sufficiently thin that there is no significant modification to the potential flow within the pipe, and that pipe curvature may be neglected. We use a local variable $\eta = a - \rho$ to describe distance from the pipe wall. The liquid velocity within the boundary layer is (u_ζ, u_η), with $u_\zeta = u_\eta = 0$ on $\eta = 0$. The unsteady boundary layer equation is

$$\frac{\partial u_\zeta}{\partial t} + u_\zeta \frac{\partial u_\zeta}{\partial \zeta} + u_\eta \frac{\partial u_\zeta}{\partial \eta} - \nu \frac{\partial^2 u_\zeta}{\partial \eta^2} = -\frac{1}{\rho_l}\frac{\partial p}{\partial \zeta}, \tag{41}$$

where p is the pressure. In the irrotational core the wall velocity $U_{\zeta w}$ satisfies

$$\frac{\partial U_{\zeta w}}{\partial t} + U_{\zeta w}\frac{\partial U_{\zeta w}}{\partial \zeta} = -\frac{1}{\rho_l}\frac{\partial p}{\partial \zeta}. \tag{42}$$

The velocity $U_{\zeta w}$ outside the boundary layer is a function only of $z = \zeta + v_0 t$. Hence

$$\begin{aligned} -\frac{1}{\rho_l}\frac{\partial p}{\partial \zeta} &= v_0 \frac{\mathrm{d}U_{zw}}{\mathrm{d}z} + U_{\zeta w}\frac{\mathrm{d}U_{zw}}{\mathrm{d}z} \\ &= U_{zw}\frac{\mathrm{d}U_{zw}}{\mathrm{d}z}, \end{aligned} \tag{43}$$

as would be found immediately by considering potential flow in the frame in which the bubble is at rest. We similarly expect the fluid velocity within the boundary layer to be a function only of (z, η), so that the boundary layer equation becomes

$$(u_\zeta + v_0)\frac{\partial u_\zeta(z,\eta)}{\partial z} + u_\eta \frac{\partial u_\zeta}{\partial \eta} - \nu \frac{\partial^2 u_\zeta}{\partial \eta^2} = U_{zw}\frac{\mathrm{d}U_{zw}}{\mathrm{d}z} \tag{44}$$

with boundary conditions

$$u_\zeta = u_\eta = 0, \quad \eta = 0, \tag{45a}$$

$$u_\eta \to 0, \quad \eta \to \infty, \tag{45b}$$

$$u_\zeta \to U_{zw}(\zeta + v_0 t) - v_0, \quad \eta \to \infty. \tag{45c}$$

Far upstream or downstream of the bubble, $|u_\zeta| \ll v_0$ and $|u_\eta|$ is similarly small. The boundary layer equation reduces to

$$v_0 \frac{\partial u_\zeta(z,\eta)}{\partial z} - \nu \frac{\partial^2 u_\zeta}{\partial \eta^2} = v_0 \frac{\mathrm{d}U_{zw}}{\mathrm{d}z} \tag{46}$$

which we re-write as

$$v_0 \frac{\partial W(z,\eta)}{\partial z} = \nu \frac{\partial^2 W(z,\eta)}{\partial \eta^2}, \tag{47}$$

where

$$W(z,\eta) = -u_\zeta(z,\eta) + U_{zw} - v_0 \tag{48}$$

with boundary conditions

$$W = U_{zw}(z) - v_0 = W_0(z), \quad \eta = 0, \tag{49a}$$

$$W \to 0, \quad \eta \to \infty. \tag{49b}$$

Equation (47) is the diffusion equation for one-dimensional motion of fluid, initially at rest, adjacent to a flat plate which translates (within its own plane) at velocity given by (49a), and z plays the role usually adopted by a time-like variable. When the bubble is still far away from any position ζ the convective terms in the equation of motion may be neglected, and an observer at the wall merely sees a time-varying bulk fluid velocity outside the boundary layer due to the approaching bubble.

When, as assumed here, $q \ll 1$ the maximum velocity (24) at the wall is $W_0 \approx 1.8 v_0 q^3 \ll v_0$, so that the diffusion equation (47) is a valid approximation to the boundary layer equation (44) everywhere, rather than just far upstream or downstream.

The solution to (47) is [20]

$$W = \eta \left(\frac{v_0}{4\pi\nu} \right)^{1/2} \int_{-\infty}^{z} W_0(\lambda) \frac{\exp[-\eta^2 v_0 / 4\nu(z-\lambda)]}{(z-\lambda)^{3/2}} \, \mathrm{d}\lambda \tag{50}$$

which, on making the substitution

$$\eta \left[\frac{v_0}{4\nu(z-\lambda)} \right]^{1/2} = \xi \tag{51}$$

reduces to

$$W = \frac{2}{\pi^{1/2}} \int_0^\infty W_0 \left(z - \frac{v_0 \eta^2}{4\nu\xi^2} \right) \mathrm{e}^{-\xi^2} \, \mathrm{d}\xi. \tag{52}$$

Straightforward substitution shows that (50) is a solution of (47), and from (52) we see that the boundary condition at $\eta = 0$ is satisfied.

6.2. Upstream asymptotics

Consider now the region $z < 0$ upstream of the bubble. If

$$W_0(z) = \mathrm{e}^{k_r z} \tag{53}$$

then using the result ([21], equation 3.325)

$$\int_0^\infty \exp\left[-at^2 - \frac{b}{t^2}\right] \mathrm{d}t = \left(\frac{\pi}{4a}\right)^{1/2} \exp\left[-2(ab)^{1/2}\right], \quad a > 0, \quad b > 0, \tag{54}$$

we have from (52)

$$W = \frac{2\mathrm{e}^{k_r z}}{\pi^{1/2}} \int_0^\infty \exp\left(-\frac{k_r v_0 \eta^2}{4\nu\xi^2} - \xi^2\right) \mathrm{d}\xi = \exp\left[k_r z - \left(\frac{k_r v_0 \eta^2}{\nu}\right)^{1/2}\right], \tag{55}$$

a similarity solution which could have been obtained directly from (47). Therefore if, by (19),

$$W_0 = U_{zw} - v_0 = v_0 \sum_{r=1}^{\infty} \frac{2b^3 C_0 k_r \mathrm{e}^{k_r z}}{3a^2 J_0(k_r a)} \tag{56}$$

then

$$u_\zeta = -W + W_0 = -\frac{2v_0 b^3 C_0}{3a^2} \sum_{r=1}^{\infty} \frac{k_r \mathrm{e}^{k_r z}}{J_0(k_r a)} \left\{ \exp\left[-\left(\frac{k_r v_0 \eta^2}{\nu}\right)^{1/2}\right] - 1 \right\}. \tag{57}$$

When $-k_0 z \gg 1$, far upstream of the bubble,

$$\frac{\partial u_\zeta}{\partial \eta} = \frac{2v_0 b^3 C_0}{3a^2} \left(\frac{v_0}{\nu}\right)^{1/2} \sum_{r=1}^{\infty} \frac{k_r^{3/2} \mathrm{e}^{k_r z}}{J_0(k_r a)} \exp\left[-\left(\frac{k_r v_0 \eta^2}{\nu}\right)^{1/2}\right] \tag{58}$$

and the dominant contribution to the viscous dissipation is

$$\mu \left(\frac{\partial u_\zeta}{\partial \eta}\right)^2 = \frac{4\mu v_0^3 b^6 C_0^2}{9a^4 \nu} \sum_{r=1}^{\infty} \sum_{s=1}^{\infty} \frac{k_r^{3/2} k_s^{3/2} \mathrm{e}^{(k_r + k_s) z}}{J_0(k_r a) J_0(k_s a)} \exp\left[-\left(k_r^{1/2} + k_s^{1/2}\right) \left(\frac{v_0 \eta^2}{\nu}\right)^{1/2}\right]. \tag{59}$$

It is straightforward to integrate (59) from $\eta = 0$ to infinity, and the viscous dissipation is integrable as $z \to -\infty$. Azimuthal integration with respect to ϕ introduces a factor $2\pi a$. Since the k_i are $\mathrm{O}(a^{-1})$, the viscous dissipation upstream of the bubble is of order

$$\mu v_0^2 b \left(\frac{v_0 b}{\nu}\right)^{1/2} \left(\frac{b}{a}\right)^{9/2}. \tag{60}$$

Since we have assumed $q \ll 1$ the boundary layer equation (44) can be approximated by the diffusion equation (47) everywhere. The above analysis therefore breaks down only when z is sufficiently small that the asymptotic expansion (56) for W_0 fails. More generally, even if q is not small, the above similarity solution will hold sufficiently far upstream of the bubble, where the wall velocity decays exponentially. However, in this case the coefficients in the expansion (56) are incorrect, since the coefficients C_i and D_i in the asymptotic expansion (18) depend upon q.

6.3. Downstream asymptotics

It is less straightforward to estimate the dissipation as $z \to \infty$ downstream of the bubble. We first observe that the total displacement of liquid adjacent to the wall (but outside the boundary layer) may be estimated

using Darwin's theory of drift [22,23]. The bubble has volume $V_b = \frac{4}{3}\pi b^3$ and as it moves it carries with it an additional volume of liquid. If the added mass of the bubble is unaffected by the presence of the pipe walls, the total volume of the bubble and added fluid is $3V_b/2$. The motion of this total volume leads to a backwards displacement of fluid which is averaged over the area πa^2 of the pipe. The total displacement at the wall is therefore $3V_b/2\pi a^2 = 2b^3/a^2$, in agreement with direct integration of the wall velocity W_0 when $G = 1$. (Note that this argument fails when the interaction between the wall and the bubble is no longer negligible, as was found for a disc, rather than a bubble, in [23].) Hence

$$\int_{-\infty}^{\infty} U_{\zeta w}\,\mathrm{d}t = \frac{2b^3}{a^2} \tag{61}$$

and

$$\int_{-\infty}^{\infty} W_0\,\mathrm{d}z = \frac{2v_0 b^3}{a^2}. \tag{62}$$

Far downstream of the bubble the viscous boundary layer will continue to diffuse towards the centre of the pipe. However, very little vorticity will be generated at the wall once $k_1 z \gg 1$. We turn to (50), and assume that z is so large that $W_0(\lambda)$ may be approximated by a delta function with total strength given by (62). The velocity within the boundary layer may then be approximated as

$$u_\zeta \approx -W = -\left(\frac{\eta^2 v_0}{4\pi\nu z}\right)^{1/2}\left(\frac{2v_0 b^3}{a^2 z}\right)\exp\left[-\eta^2 v_0/4\nu z\right]. \tag{63}$$

Note that (63) predicts that $W = 0$ on $\eta = 0$, rather than $W = W_0(z)$. This is because the exponential tail of W_0 as $z \to \infty$ is neglected when we approximate W_0 by a delta function. We see from *figure 2* that the errors are small, since $W_0/v_0 q^3 < 2 \times 10^{-5}$ for $|z| > 2a$. Smythe showed that the potential flow decays exponentially both upstream and downstream of the bubble (17). From (63) we find that

$$\int_0^{\infty} u_\zeta\,\mathrm{d}\eta = -\frac{b^3}{a^2}\left(\frac{4\nu v_0}{\pi z}\right)^{1/2} \tag{64}$$

which decays as $z \to \infty$. The downstream decay of the (weak) bubble wake is discussed by Moore [10].

As before, we can estimate the dissipation within the boundary layer assuming that the boundary layer, though thicker than upstream of the bubble, is nevertheless still sufficiently thin that derivatives in the ζ direction may be neglected:

$$\mu\frac{\partial u_\zeta}{\partial\eta}\frac{\partial u_\zeta}{\partial\eta} = \frac{\mu v_0^3 b^6}{\pi\nu a^4 z^3}\left(1 - \frac{\eta^2 v_0}{2\nu z}\right)^2\exp\left[-\frac{\eta^2 v_0}{2\nu z}\right] \tag{65}$$

so that

$$\mu\int_0^{\infty}\frac{\partial u_\zeta}{\partial\eta}\frac{\partial u_\zeta}{\partial\eta}\,\mathrm{d}\eta = \frac{3\mu v_0^3 b^6}{8\nu a^4 z^3}\left(\frac{2\nu z}{\pi v_0}\right)^{1/2} \tag{66}$$

and this is clearly integrable as $z \to \infty$. Adopting a cut-off at $z = a$ and introducing a factor $2\pi a$ to account for integration with respect to ϕ, we find that the viscous dissipation in the trailing wake is of order

$$\mu v_0^2 b\left(\frac{v_0 b}{\nu}\right)^{1/2}\left(\frac{b}{a}\right)^{9/2} \tag{67}$$

which is identical to the order of magnitude of the upstream dissipation (60).

In the central region of length $2a$ around $z = 0$, the boundary layer has thickness of order $(a\nu/v_0)^{1/2}$ and the velocity outside the boundary layer is of order $v_0(b/a)^3$. The rate of dissipation, after integration over the relevant volume, has the same order of magnitude as the dissipation upstream (60) and downstream (67).

6.4. Numerical computations

The dissipation within the boundary layer on the walls of the pipe may be computed numerically by solving the boundary layer equation (44). Here, however, we shall assume that $q \ll 1$, so that we may solve the simpler diffusion equation (47). We make the scalings

$$\hat{z} = \frac{z}{a}, \qquad \hat{\eta} = \eta\left(\frac{v_0}{a\nu}\right)^{1/2}, \qquad \hat{W} = \frac{W}{v_0 q^3} \tag{68}$$

and in consequence $\hat{k}_r = k_r a$. The diffusion equation (47) becomes

$$\frac{\partial \hat{W}}{\partial \hat{z}} = \frac{\partial^2 \hat{W}}{\partial \hat{\eta}^2} \tag{69}$$

with initial condition

$$\hat{W} = -\sum_{r=1}^{\infty} \frac{\hat{k}_r e^{\hat{k}_r \hat{z}}}{J_0(\hat{k}_r)} \exp\left[-\hat{k}_r^{1/2}\hat{\eta}\right], \quad z \to -\infty, \tag{70}$$

and with boundary conditions (49). The diffusion equation (69) was solved numerically, and results for $\hat{W}(\hat{\eta})$ at various values of $\hat{z}$ are shown in *figure 3*. The shear rate may then be evaluated and we first obtain the integral

$$I_\eta = \int_0^\infty \left(\frac{\partial W}{\partial \eta}\right)^2 \mathrm{d}\eta = v_0^2\left(\frac{b}{a}\right)^6 \left(\frac{v_0}{a\nu}\right)^{1/2} \hat{I}_\eta, \tag{71}$$

where

$$\hat{I}_\eta = \int_0^\infty \left(\frac{\partial \hat{W}}{\partial \hat{\eta}}\right)^2 \mathrm{d}\hat{\eta}. \tag{72}$$

Curve (a) of *figure 4* shows $\hat{I}_\eta$ as a function of $\hat{z}$. Also shown on *figure 4* are asymptotes (b) based on (66) downstream of the bubble and (c) based on (59) upstream of the bubble. Note that curves (a) and (c) are indistinguishable for $\hat{z} < -0.1$.

The total rate of viscous dissipation within the boundary layer is obtained by integrating I_η with respect to z and ϕ and is

$$\begin{aligned} 2\pi a\mu \int_{-\infty}^{\infty} \mathrm{d}z \int_0^\infty \left(\frac{\partial u_\zeta}{\partial \eta}\right)^2 \mathrm{d}\eta &= 2\pi a^2 \mu v_0^2 \left(\frac{b}{a}\right)^6 \left(\frac{v_0}{a\nu}\right)^{1/2} \int_{-\infty}^{\infty} \hat{I}_\eta \,\mathrm{d}\hat{z} \\ &= 7.66\mu v_0^2 b \left(\frac{2v_0 b}{\nu}\right)^{1/2} \left(\frac{b}{a}\right)^{9/2}, \end{aligned} \tag{73}$$

where the value 7.66, obtained numerically, is thought to be accurate to within 1%.

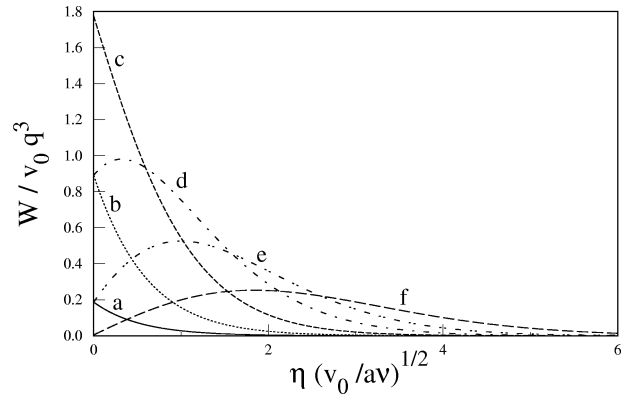

Figure 3. The liquid velocity $\hat{W}(\hat{z},\hat{\eta})$, defined by (48), within the boundary layer: (a) $\hat{z}=-1.0$; (b) $\hat{z}=-0.5$; (c) $\hat{z}=0$; (d) $\hat{z}=0.5$; (e) $\hat{z}=1.0$; (f) $\hat{z}=2.0$.

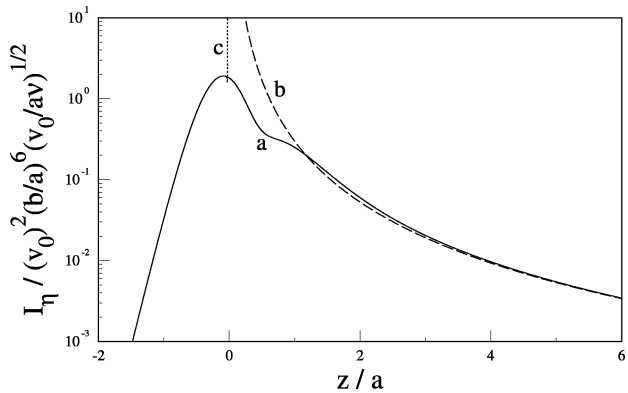

Figure 4. The integral $\hat{I}_\eta$, defined by (72), giving the local rate of dissipation as a function of $\hat{z}$. Curve (a) shows the full numerical results, (b) is the downstream asymptotic prediction (66) and (c) the upstream asymptotic prediction (59). Curve (c) is indistinguishable from (a) for $\hat{z}<-0.1$.

Adding this dissipation to that within the irrotational core evaluated in section 5 we obtain the total dissipation within the liquid surrounding the bubble. The rate of working at the pipe walls is zero, as in section 5, since although we now admit a tangential stress the liquid velocity at the wall is zero. Hence the rate of dissipation must again equal the rate of working by the drag force D acting on the bubble, so that

$$D = 12\pi\mu v_0 b\left[1-\frac{2.21}{\mathrm{Re}^{1/2}}+\mathrm{O}\left(\mathrm{Re}^{-5/6}\right)\right]\left(1+1.5936q^3\right)+7.66\mu v_0 b\mathrm{Re}^{1/2}q^{9/2}. \tag{74}$$

The contribution to the drag due to the boundary layer differs from that in the irrotational core by a factor of order $\mathrm{Re}^{1/2}q^{9/2}$ and could dominate in the limit $\mathrm{Re}\to\infty$. As discussed in section 1, Moore showed that once the bubble Reynolds number is large the bubble deforms and the expressions (4) and (5) for the drag D are in poor agreement with experiment once the radius of air bubble rising in water becomes larger than about 0.5 mm. Moore's analysis [8] of distorted bubbles extends the range of agreement only slightly [8,24]. Taking $\rho_l=1000$ kgm^{-3}, $\mu=10^{-3}$ Pas and $b=0.5$ mm, Levich (4) predicts a rate of rise $v_0=0.27$ ms^{-1} and a Reynolds number $2v_0b/\nu=270$. Thus if $q\ll 1$ the viscous boundary layer at the pipe walls will have a negligible effect on the rate of rise of an air bubble in water. From (3) we see that larger Reynolds numbers might be achieved in fluids for which the Morton number (2) is small. However, there is not much scope

for reducing M: the lowest values reported by Harper [25] are $M < 10^{-13}$ for liquid metals. Smaller Morton numbers, and hence, by (3), larger Reynolds numbers, may be possible for spherical bubbles rising in a low gravity environment, assuming that the bubble remains stable.

6.5. The pressure on the bubble

All the analysis here has been in terms of the dissipation within the fluid, and we might ask how the dissipation within the boundary layer would show up in a direct computation of the forces acting over the surface of the bubble.

The displacement thickness L of the pipe wall boundary layer is of order $L = \mathrm{O}(\nu a/v_0)^{1/2}$ in the vicinity of the bubble $z = 0$. This reduces the effective radius of the pipe. The shear rate at the surface of a bubble in unbounded potential flow is $\mathrm{O}(v_0/b)$, and the results of section 4 indicate that in the pipe this is increased by a factor $G = 1 + 0.797(b/a)^3$. The force acting on the bubble is therefore $\mathrm{O}(\mu v_0 bG)$ and will change by an amount $\mathrm{O}(\mu v_0 bq^{7/2}\mathrm{Re}^{-1/2})$ if a changes by a small amount $L \sim (\nu a/v_0)^{1/2}$. This correction is smaller than the $\mathrm{O}(\mu v_0 bq^3\mathrm{Re}^{-1/2})$ correction to Moore's drag (35) found in section 5.2. It is also quite different from the $\mathrm{O}(\mu v_0 bq^{9/2}\mathrm{Re}^{1/2})$ correction to the drag predicted in (74).

In order to understand the drag predicted by energy arguments, we note that the displacement thickness of the boundary layer on the pipe wall increases in the downstream direction. When we allow for the effect of the varying displacement thickness we destroy the upstream-downstream symmetry of the potential flow. The potential-flow pressures on the upstream and downstream surfaces of the bubble no longer cancel, and we now estimate the magnitude of this effect.

In the frame in which the bubble is at rest, the tangential velocity over the bubble surface is given by (27) so that the perturbation in the pressure over the surface of the bubble due to the walls of the pipe is of order $\rho_l v_0^2 (b/a)^3$. If the effective pipe radius changes by Δa between the upstream and downstream sides of the bubble, the pressure changes by an amount of order $\rho_l v_0^2 b^3 \Delta a/a^4$ and this pressure acts over an area of order b^2. If the boundary layer thickness is $L \sim (\nu a/v_0)^{1/2}$, then on dimensional grounds we expect the change in boundary layer thickness ΔL in a time Δt due to diffusion to be of order $\nu \Delta t/L$. We identify Δt with the timescale b/v_0 for the bubble to pass any point, and we identify the effective change in pipe radius Δa with the change in boundary layer thickness ΔL. This leads to an estimate of the pressure force which is of order $b^6 \mu v_0 a^{-4} (v_0/\nu a)^{1/2}$, which corresponds to the estimated rate of dissipation (60) within the boundary layer.

7. Concluding remarks

The effect of pipe diameter on the drag predicted by (74) is much smaller than the experimental correlation (6), which includes not only the gas bubble results of Uno and Kintner [26], but also many results for the velocity of liquid droplets. Moreover, on comparison with Duineveld's results for air bubbles rising through pure water [24], it would appear that the results of [26] pertain either to large, non-spherical bubbles, or to small bubbles which behave as rigid spheres due to the effect of surface contaminants, as discussed in [13,25, 27]. It can be seen both from the composite plot in figure 9.8 of [13] and from the results in figure 10 of Uno and Kintner [26] that there is considerable experimental scatter when $q \ll 1$. Experiments in fluids other than water would reduce the effects of surface contaminants, and the predicted drag (74) would provide a rational theory against which such experimental results could be compared. Although numerical studies of bubbles rising in tubes at high Reynolds numbers have been published for bubbles and tubes having similar diameters, I have been unable to find any such studies for the case in which the bubble diameter is small compared to that of the pipe.

The drag (35), which allows slip at the walls of the container, indicates the errors which might be expected to occur when computing the high Reynolds number drag on a bubble using a finite (rather than infinite) computational domain. Thus in [17] the computational domain corresponded approximately to a cylinder of radius $a = 80b$, and errors of order 0.0003% would have been negligible. Note that at the pipe wall the normal velocity $u_\rho = 0$, so that $\partial u_\rho/\partial z = 0$ at $\rho = a$. If the flow is irrotational we conclude that $\partial u_z/\partial\rho = 0$ at $\rho = a$ and a stress-free boundary condition at the cylindrical wall is therefore satisfied exactly by the potential flow. A weak boundary layer adjusts the shear-rate at the stress-free surface of the bubble, but no such boundary layer is required at the stress-free outer cylindrical boundary.

Acknowledgements

I thank several anonymous refereees for helpful suggestions, and Professor Howard Stone for discussions supported by the NATO Collaborative Research Grant Programme (CRG.961165).

References

[1] Soubiran J., Sherwood J.D., Bubble motion in a potential flow within a Venturi, Int. J. Multiphase Flow 26 (2000) 1771–1796.
[2] Sherwood J.D., Potential flow around a deforming bubble in a Venturi, Int. J. Multiphase Flow 26 (2000) 2005–2047.
[3] Smythe W.R., Flow around a sphere in a circular tube, Phys. Fluids 4 (1961) 756–759.
[4] Smythe W.R., Flow around a spheroid in a circular tube, Phys. Fluids 7 (1964) 633–638.
[5] Cai X., Wallis G.B., Potential flow around a row of spheres in a circular tube, Phys. Fluids A 4 (1992) 904–912.
[6] Hartunian R.A., Sears W.R., On the instability of small gas bubbles moving uniformly in various liquids, J. Fluid Mech. 3 (1957) 27–47.
[7] Moore D.W., The rise of a gas bubble in a viscous liquid, J. Fluid Mech. 6 (1959) 113–130.
[8] Moore D.W., The velocity of rise of distorted gas bubbles in a liquid of small viscosity, J. Fluid Mech. 23 (1965) 749–766.
[9] Haberman W.L., Morton R.K., An experimental investigation of the drag and shape of air bubbles rising in various liquids, David Taylor Model Basin, Report no. 802, 1953.
[10] Moore D.W., The boundary layer on a spherical gas bubble, J. Fluid Mech. 16 (1963) 161–176.
[11] Levich V., Motion of gaseous bubbles with high Reynolds numbers, Zh. Eksp. Teor. Fiz. 19 (1949) 18–24 (in Russian).
[12] Kang I.S., Leal L.G., The drag coefficient for a spherical bubble in a uniform streaming flow, Phys. Fluids 31 (1988) 233–237.
[13] Clift R., Grace J.R., Weber M.E., Bubbles, Drops and Particles, Academic Press, New York, 1978.
[14] Maxworthy T., Gnann C., Kürten M., Durst F., Experiments on the rise of air bubbles in clean viscous liquids, J. Fluid Mech. 321 (1996) 421–441.
[15] Ryskin G., Leal L.G., Numerical solution of free-boundary problems in fluid mechanics, J. Fluid Mech. 148 (1984) 1–17.
[16] Brabston D.C., Keller H.B., Viscous flows past spherical gas bubbles, J. Fluid Mech. 69 (1975) 179–189.
[17] Magnaudet J., Rivero M., Fabre J., Accelerated flows past a rigid sphere or a spherical bubble. Part I. Steady straining flow, J. Fluid Mech. 284 (1995) 97–135.
[18] Oguz H.N., Prosperetti A., The natural frequency of oscillation of gas bubbles in tubes, J. Acoust. Soc. Am. 103 (1998) 3301–3308.
[19] Batchelor G.K., An Introduction to Fluid Dynamics, Cabridge University Press, Cambridge, 1973.
[20] Carslaw H.S., Jaeger J.C., Conduction of Heat in Solids, 2nd ed., Oxford University Press, Oxford, 1959.
[21] Gradshteyn I.S., Ryzhik I.M., Table of Integrals, Series, and Products, Academic Press, 1980.
[22] Eames I., Belcher S.E., Hunt J.C.R., Drift, partial drift and Darwin's proposition, J. Fluid Mech. 275 (1994) 201–223.
[23] Sherwood J.D., Stone H.A., Added mass of a disc accelerating within a pipe, Phys. Fluids 9 (1997) 3141–3148.
[24] Duineveld P.C., The rise velocity and shape of bubbles in pure water at high Reynolds number, J. Fluid Mech. 292 (1995) 325–332.
[25] Harper J.F., The motion of bubbles and drops through liquids, Adv. Appl. Mech. 12 (1972) 59–129.
[26] Uno S., Kintner R.C., Effect of wall proximity on the rate of rise of single air bubbles in a quiescent liquid, A.I.Ch.E. J. 2 (1956) 420–425.
[27] Magnaudet J., Eames I., The motion of high-Reynolds-number bubbles in inhomogeneous flows, Annu. Rev. Fluid Mech. 32 (2000) 659–708.